Magnetic Resonance in Medicine 64:767–776 (2010)

Combination of Compressed Sensing and Parallel Imaging for Highly Accelerated First-Pass Cardiac Perfusion MRI

Ricardo Otazo,* Daniel Kim, Leon Axel, and Daniel K. Sodickson

First-pass cardiac perfusion MRI is a natural candidate for compressed sensing acceleration since its representation in the combined temporal Fourier and spatial domain is sparse and the required incoherence can be effectively accomplished by *k-t* random undersampling. However, the required number of samples in practice (three to five times the number of sparse coefficients) limits the acceleration for compressed sensing alone. Parallel imaging may also be used to accelerate cardiac perfusion MRI, with acceleration factors ultimately limited by noise amplification. In this work, compressed sensing and parallel imaging are combined by merging the *k-t* SPARSE technique with sensitivity encoding (SENSE) reconstruction to substantially increase the acceleration rate for perfusion imaging. We also present a new theoretical framework for understanding the combination of *k-t* SPARSE with SENSE based on distributed compressed sensing theory. This framework, which identifies parallel imaging as a distributed multisensor implementation of compressed sensing, enables an estimate of feasible acceleration for the combined approach. We demonstrate feasibility of 8-fold acceleration in vivo with whole-heart coverage and high spatial and temporal resolution using standard coil arrays. The method is relatively insensitive to respiratory motion artifacts and presents similar temporal fidelity and image quality when compared to Generalized autocalibrating partially parallel acquisitions (GRAPPA) with 2-fold acceleration. Magn Reson Med 64:767–776, 2010. © 2010 Wiley-Liss, Inc.

Key words: compressed sensing; parallel imaging: joint sparsity; dynamic imaging; cardiac perfusion

First-pass cardiac perfusion MRI is a promising and much-studied modality for noninvasive assessment of coronary artery disease (1,2). However, robust implementation for routine clinical use can be technically challenging. In particular, the pulse sequence must be carefully designed to balance conflicting requirements, such as spatial resolution, temporal resolution, contrast-to-noise ratio, and spatial coverage. Currently, parallel imaging techniques for dynamic MRI, such as temporal SENSE (TSENSE) (3) and temporal GRAPPA (TGRAPPA) (4), can be used to acquire three to four slices per heartbeat, with adequate spatial and temporal resolution for clinical interpretation, using commercially available radiofrequency coil arrays.

Center for Biomedical Imaging, Department of Radiology, New York University School of Medicine, New York, New York, USA.

Grant sponsor: National Institutes of Health; Grant numbers: R01-EB000447, R01-HL083309; Grant sponsor: American Heart Association; Grant number: AHA0730143N.

*Correspondence to: Ricardo Otazo, Ph.D., Center for Biomedical Imaging, Department of Radiology, New York University School of Medicine, 660 First Ave, 4th Floor, New York, NY. E-mail: ricardo.otazo@nyumc.org

Received 17 July 2009; revised 22 February 2010; accepted 24 February 2010.

DOI 10.1002/mrm.22463
Published online 9 June 2010 in Wiley Online Library (wileyonlinelibrary.com).

To extend the slice coverage and/or increase spatial and temporal resolution, more advanced techniques are needed to obtain higher acceleration factors. Such techniques include *k-t* Broad-use linear acquisition speed-up technique (BLAST) and *k-t* SENSE (5), *k-t* GRAPPA (6), and SPatiotemporal domain-based unaliasing employing sensitivity Encoding and Adaptive Regularization (SPEAR) (7), which exploit spatiotemporal correlations in the dynamic MRI data either alone or in combination with coil sensitivity information. In these methods, the k_y-t space signal is sampled on a sheared grid, which results in reduced signal overlap in the sparse temporal Fourier domain (*y-f*), and as a result higher undersampling rates are feasible. However, dynamic training data are required to establish an aliasing pattern in the *y-f* domain, which reduces the effective acceleration rate. For perfusion imaging, training data must be interleaved with undersampled imaging data to reflect similar contrast enhancement and avoid misregistration due to respiratory motion. Previously described perfusion studies using *k-t* techniques have reported acceleration factors greater than 6 (8–10). However, respiratory motion represents a source of reconstruction error for these techniques, since signal overlap increases in the *y-f* domain due to the presence of higher temporal frequencies and results in residual aliasing artifacts.

An alternative method for reconstruction of undersampled data is compressed sensing, which is based upon the principle that an image with a sparse representation in a known transform domain can be recovered from randomly undersampled *k*-space data, using a nonlinear reconstruction (11). Unlike *k-t* BLAST and *k-t* SENSE, compressed sensing does not require training data, and, as a result, it may be less sensitive to inconsistencies between training and imaging data. Application of compressed sensing to dynamic MR imaging has been presented in methods such as *k-t* SPARSE (12), compressed sensing dynamic imaging (13), and *k-t* FOCUSS (14), using the temporal FFT as the sparsifying transform (*y-f* space as the sparse domain) and k_y-t random undersampling. However, the maximum acceleration rate reported by a previous first-pass cardiac perfusion study employing the method described in Gamper et al. (13) was only 4 (15).

Maximum acceleration rate in compressed sensing is determined by image sparsity. In practice, the number of required samples is approximately three to five times the number of nonzero coefficients in the image or in some appropriate transform domain (11,16). When multiple receiver coils are employed, compressed sensing can be combined with parallel imaging techniques (17–19) to

obtain higher accelerations. Previous combinations for nondynamic MRI have framed compressed sensing as a regularization method for parallel imaging reconstructions such as SENSE and have demonstrated increased acceleration capability over each of the techniques applied separately (20–23). Another method applied coil-by-coil compressed sensing to reconstruct regularly aliased images and then used standard SENSE reconstruction to remove the aliasing (24). This two-step approach, however, runs the risk of inefficiency since correlations between coils are only used at the second step. The recently introduced theory of distributed compressed sensing (25) extends compressed sensing to include multiple sensors in order to reduce the number of required samples by exploiting the idea of joint sparsity in the multisignal ensemble rather than simply exploiting separate sparsity.

In this work, a combination of the *k-t* SPARSE and SENSE techniques is employed for highly accelerated first-pass cardiac perfusion imaging using a temporal Fourier transform as the sparsifying transform. It is demonstrated that this approach represents a form of distributed compressed sensing, exploiting joint sparsity in multicoil images rather than coil-by-coil sparsity (26,27). Using the theoretical framework of distributed compressed sensing, estimates of maximum feasible accelerations for the combination of *k-t* SPARSE and SENSE are derived. For experimental validation of the maximum practical acceleration rate, fully sampled, first-pass cardiac perfusion MRI data were acquired in vivo and then undersampled to various degrees. Highly accelerated in vivo perfusion data were then acquired and reconstructed to demonstrate the feasibility of the method. Sensitivity to respiratory motion was evaluated in terms of residual aliasing artifacts. A comparison of the proposed method at 8-fold acceleration with commercially available GRAPPA at 2-fold acceleration was performed to evaluate their relative performance. Finally, 8-fold accelerated *k-t* SPARSE-SENSE images were obtained in a patient with acute myocardial infarction.

THEORY

Compressed Sensing for First-Pass Cardiac Perfusion MRI

The requirements for a successful application of compressed sensing are (a) image sparsity in a known transform domain, i.e., few large coefficients and many small coefficients that can be omitted without loss of image quality; (b) incoherent undersampling artifacts in the sparse domain, i.e., the undersampling artifacts look like additive noise; and (c) nonlinear reconstruction to recover the sparse coefficients. The cardiac perfusion signal is sparse in the combined temporal Fourier and spatial domain (*y-f* space) since only portions of the field of view require the full temporal bandwidth and the other regions have only static information or at low temporal frequencies (Fig. 1). The required incoherence can be obtained by randomly omitting phase-encoding lines (k_y) with a different pattern for each time point (t), generating a random undersampling pattern in k_y-t space. Compared with k_y-only random undersampling, k_y-t random undersampling increases the incoherence since the undersampling artifacts are incoherently distributed along two dimensions rather than one.

Combination of Compressed Sensing and Parallel Imaging

The perfusion data (in k_x-k_y-t space) acquired in each coil can be represented as:

$$\mathbf{m}_l = \mathbf{F}^s \mathbf{S}_l \mathbf{d}, \quad [1]$$

where $\mathbf{d}$ is the perfusion image series to be reconstructed in x-y-t space, $\mathbf{F}^s$ is the spatial Fourier transform, and $\mathbf{S}_l$ represents the coil sensitivities (in x-y space). Note that k_x is fully sampled. Instead of applying compressed sensing to each coil separately, the multicoil SENSE model given by the concatenation of the individual models is solved:

$$\mathbf{m} = \mathbf{E}\mathbf{d}, \quad [2]$$

where $\mathbf{m} = \begin{bmatrix} \mathbf{m}_1 \\ \vdots \\ \mathbf{m}_{N_c} \end{bmatrix}, \mathbf{E} = \mathbf{F}^s \begin{bmatrix} \mathbf{S}_1 \\ \vdots \\ \mathbf{S}_{N_c} \end{bmatrix}$ and N_c is the number of coils. The compressed sensing reconstruction of the SENSE model is given by:

$$\hat{\mathbf{d}} = \arg\min_{\mathbf{d}} \left\{ \|\mathbf{E}\mathbf{d} - \mathbf{m}\|_2^2 + \lambda \left\| \mathbf{F}^t \mathbf{d} \right\|_1 \right\}, \quad [3]$$

where $\mathbf{F}^t$ is the temporal Fourier transform, $\|\cdot\|_1$ is the l_1-norm or sum of absolute values given by $\|\mathbf{x}\|_1 = \sum_i |x_i|$, and $\|\cdot\|_2$ is the l_2-norm given by $\|\mathbf{x}\|_2 = \left(\sum_i |x_i|^2\right)^{\frac{1}{2}}$. The l_1-norm term enforces sparsity in the temporal Fourier domain, and the l_2-norm term enforces data consistency with a model error threshold, given by ε (ε is usually set to the noise level). λ Is a weighting parameter that controls the balance between sparsity in the temporal Fourier domain (right-hand term) and parallel imaging data consistency (left-hand term). The reconstruction problem associated with Eq. 3 represents a combination of *k-t* SPARSE and SENSE using a temporal FFT as sparsifying transform.

Distributed Compressed Sensing Framework

Previous combinations of compressed sensing and parallel imaging have presented compressed sensing as a nonlinear regularizer for SENSE reconstruction (20–23). Even though the *k-t*-domain reconstruction problem in Eq. 3 may be solved in practice with regularized techniques such as a nonlinear conjugate gradient algorithm (see Materials and Methods), it is difficult from this perspective to estimate theoretical bounds for the expected feasible acceleration. In this work, we present a new framework for combinations of compressed sensing and parallel imaging based on distributed compressed theory (25), in order to assess theoretical bounds on the maximal acceleration.

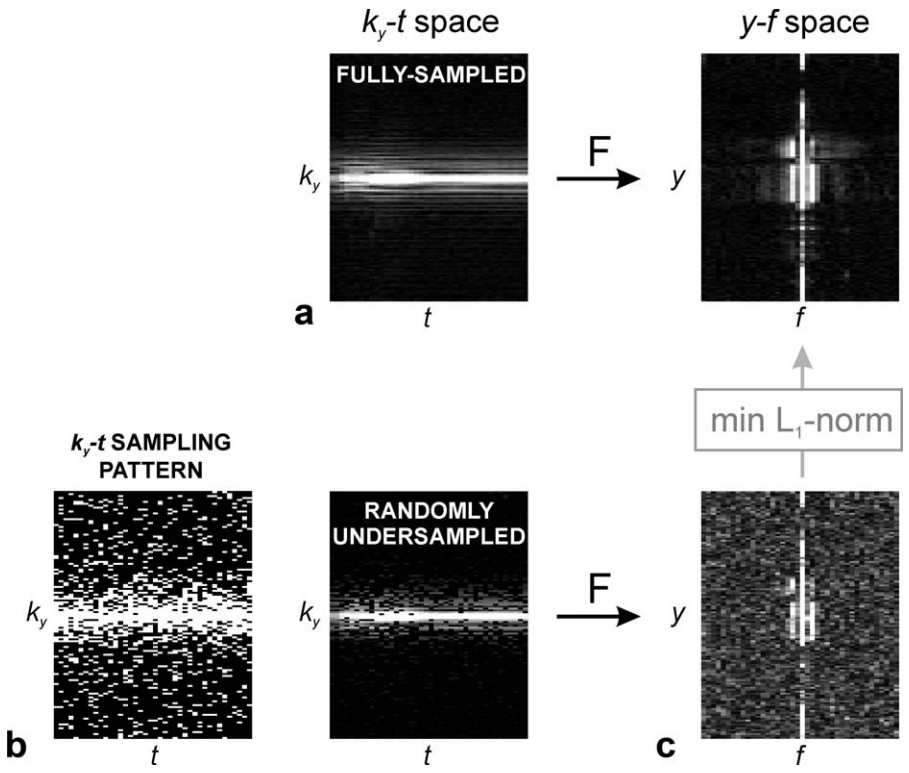

FIG. 1. Conceptual illustration of the compressed sensing technique for cardiac perfusion MRI. **a:** Sparsity: the fully sampled k_y-t data are sparse in y-f space. **b:** Incoherence: k_y-t pseudorandom undersampling preserves the original sparse representation in y-f space and presents artifacts that look like additive noise (pseudonoise). **c:** Nonlinear reconstruction: the sparse coefficients in y-f space can be recovered with a nonlinear reconstruction that minimizes the number of nonzero coefficients (minimum L_1-norm).

The combination of k-t SPARSE and SENSE does indeed represent a form of distributed compressed sensing since joint sparsity is exploited instead of individual coil-by-coil sparsity to reconstruct one image series (**d** in Eqs. 1–3 above) that represents the combination from all coils. In a general sense, one might expect that enforcing joint sparsity would reduce the number of required samples per coil and add incoherence to the problem. First of all, the signal sampled by each coil is given by the convolution in k-space of the object function and the k-space representation of the spatial coil sensitivity. Therefore, multicoil samples with different spatial information content are simultaneously obtained to reduce the required number of samples per coil needed to reconstruct an unaliased image, just as in parallel imaging (17–19). Second of all, even though the same k_y-t random undersampling pattern is shared for all coils, the convolution in k-space with the coil sensitivities will generate different incoherent artifacts for each coil.

The theory of distributed compressed sensing enables one to place concrete bounds on this intuitive expectation. In practice, the number of required samples to perform accurate reconstructions in compressed sensing alone using l_1-norm minimization is three to five times the number of sparse coefficients K (3-5K) (11,16). It has been shown, however, that for a distributed compressed sensing model with a large number of sensors (25), the number of required samples approaches K when different random undersampling patterns are used for each sensor. At first glance, it is not obvious that the case of multicoil acquisition in MR meets this condition, since signals from all coils share the same gradient-based undersampling pattern, albeit convolved with distinct coil sensitivity patterns. One might therefore expect a reduction in incoherence and a departure from the theoretical bounds on signal recovery outlined in (25). Fortunately, however, parallel imaging itself provides the tools needed to match in practice the theoretical condition of distinct random undersampling. At the core of parallel imaging is a principle of physical regridding, in which signals acquired in multiple coils are recombined to generate signals shifted by some amount in k-space. Using techniques like the grappa operating gridding method (28), sets of distinct combinations may in fact be chosen to synthesize signals for new virtual "coils," each with a different random undersampling profile. The price to pay for such physical regridding using parallel imaging would be some loss in signal-to-noise ratio, which would be modest in this case since no large shifts in k-space are required to synthesize a k-space pattern that is effectively uncorrelated with the starting pattern, particularly when large numbers of coils are used. In any case, we are not proposing recombination to virtual uncorrelated coils as a practical reconstruction technique, but rather as a means of demonstrating that the combination of compressed sensing and parallel imaging meets the conditions of distinct random undersampling (25). We may therefore have some confidence (pending formal mathematical proof of the statistical robustness of reconstruction with virtual uncorrelated coils) that the corresponding limits on accurate recovery of signal in the noise-free case may apply.

Our own work (26) has also demonstrated in practice that increasing the number of coils reduces the required number of samples for accurate combined compressed sensing and parallel imaging reconstruction to a minimum of K. The maximum increase in acceleration that may reasonably be expected by combining parallel

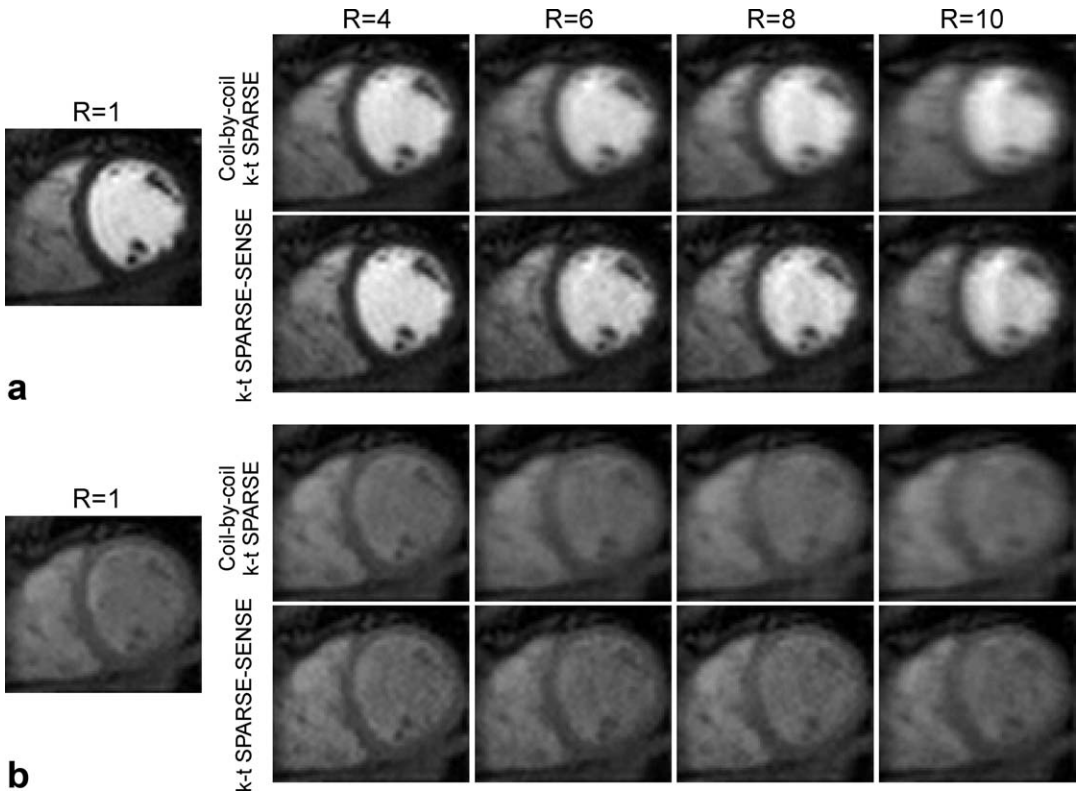

FIG. 2. Fourier reconstruction of the fully sampled data ($R = 1$), coil-by-coil compressed sensing (coil-by-coil *k-t* SPARSE) and *k-t* SPARSE-SENSE reconstruction with simulated acceleration factors of $R = 4$, 6, 8, and 10 for **(a)** peak blood enhancement and **(b)** peak myocardial wall enhancement.

imaging with compressed sensing compared with using compressed sensing alone is then about 3- to 5-fold for large numbers of coils. Of course, the baseline degree of acceleration possible with compressed sensing alone depends upon the level of sparsity of the underlying images in each coil. The maximum additional factor of 3 to 5 with parallel imaging represents an upper bound to what parallel imaging can add to the information that is already present inherently in a coil-by-coil compressed sensing reconstruction.

MATERIALS AND METHODS

Data Acquisition

First-pass cardiac perfusion MRI was performed on two healthy volunteers (two males; ages 32 and 23 years) and one patient (male, age 38 years), with 0.1 mmol/kg of gadopentetate-dimeglumine (Magnevist, Bayer Healthcare, Leverkusen, Germany). The patient presented with chest pain, electrocardiogram changes, and elevated troponin (peak 52 ng/mL) 6 days prior to MRI. Diagnostic catheterization showed total occlusion of the left posterior descending artery, but revascularization was not performed because the occluded vessel was small in caliber, very distal, and had collateral flow from other vessels. Human imaging was performed in accordance with protocols approved by the institutional review board at the New York University School of Medicine, and all subjects provided written informed consent.

Data were acquired with a modified TurboFLASH pulse sequence on a whole-body 3-T scanner (Tim Trio; Siemens Healthcare, Erlangen, Germany). The radiofrequency excitation was performed using the transmit body coil, and six anterior elements and six posterior elements of the Siemens body matrix array were used for signal reception.

In one volunteer, a fully sampled perfusion image acquisition was performed in a midventricular short-axis location at mid diastole (trigger delay 400 ms) with an image matrix of 128×128. This data set was used as a template to simulate acceleration rates $R = 4$, 6, 8, 10, and 12 (Fig. 2). The relevant imaging parameters include field of view = $320 \times 320\text{mm}^2$, slice-thickness = 8mm, flip angle = 10°, echo time/pulse repetition time = 1.2/2.4 ms, bandwidth = 1000 Hz/pixel, radiofrequency pulse train saturation pulse (29), delay time = 10 ms, repetitions = 40, spatial resolution = $3.2 \times 3.2\text{mm}^2$, and temporal resolution = 307 ms.

In a separate experiment, an 8-fold accelerated multislice acquisition with user-defined phase-encoding and temporal (k_y-t) sampling patterns was performed using the same set of imaging parameters with the following exceptions: image matrix = 192×192, spatial resolution = $1.67 \times 1.67\text{mm}^2$, echo time/pulse repetition time = 1.3/2.5 ms, and temporal resolution = 60 ms. $R = 8$ was chosen based on the simulated acceleration results, which are presented below. Low-spatial-resolution coil-sensitivity data were acquired during the first heartbeat, using an image acquisition matrix of 64×24.

Acceleration was accomplished using k_y-t random undersampling with variable k-space trajectory, where the undersampling pattern along k_y was varied as a function of time in order to produce the required incoherence of artifacts in the sparse y-f domain (Fig. 1). Sampling more densely at the center of k_y-space increases incoherence and provides a better starting point for reconstruction than uniform random sampling (11). The k_y sampling was performed using a reverse-centric k-space reordering in order to increase the contrast-to-noise ratio, at the expense of slight blurring in the k_y direction (30). During the first injection of gadopentetate-dimeglumine (0.1 mmol/kg at 6 mL/sec, with a 20-mL saline flush), 10 short-axis slices were acquired within a breath hold. After 20 min, during the second injection of gadopentetate-dimeglumine (the same parameters as for first injection), a repeated scan was performed under heavy breathing in order to evaluate the sensitivity to respiratory motion.

In another volunteer, comparison between k-t SPARSE-SENSE with $R = 8$ and commercially available GRAPPA (19) with $R = 2$ was performed by interleaving SPARSE-SENSE and GRAPPA acquisitions within the same heartbeat. This acquisition scheme enabled comparison of the image quality with identical contrast agent concentration, slice position, and image scale factors. The TD of both acquisitions was varied to keep the same effective recovery time of magnetization between the saturation pulse and the center of k-space acquisition. The relevant imaging parameters included image acquisition matrix = 128 × 128, spatial resolution = 3.2 × 3.2mm^2, and temporal resolution = 38.4/173 ms for k-t SPARSE-SENSE/GRAPPA, respectively.

In the patient with myocardial infarction, the 8-fold accelerated k-t SPARSE-SENSE acquisition was performed using the same parameters as in the breath-held volunteer study. Delayed-enhancement images were obtained using a phase-sensitive inversion recovery (31) pulse sequence 15 min after the administration of the contrast agent.

Acceleration Analysis

Estimates of expected feasible accelerations were computed using the fully sampled data set. The maximum compression ratio provided by the temporal fast Fourier transform (FFT) was assessed by truncating the representation of the fully sampled data in x-y-f space and computing the difference with the full representation in the x-y-t domain. A threshold of 5% root mean square error was used to establish the maximum compression ratio. The maximum feasible acceleration for compressed sensing alone was then estimated to lie between compression ratio^{max}/3 and compression ratio^{max}/5. The increase in acceleration provided by the combination with parallel imaging was assessed by reconstructing the fully sampled data set with simulated accelerations and comparing with the original data.

Image Reconstruction

Combination of k-t SPARSE and SENSE was implemented in MatLab (The MathWorks, Natick, MA) by extending the SparseMRI method (11) to include the time dimension and the coil sensitivities in the acquisition model and to enforce joint sparsity in the reconstruction. A nonlinear conjugate gradient algorithm (11) was employed to solve the minimization problem given in Eq. 3, where the l_1-term was computed using the sensitivity-weighted multicoil image combination (32). The matrix **E** was not computed explicitly and was replaced by FFT and matrix-vector multiplications, just as in the conjugate-gradient SENSE method (33). The starting point of the nonlinear conjugate gradient algorithm was given by the sensitivity-weighted multicoil image combination of the zero-filled Fourier reconstruction.

The weighting parameter (λ) in Eq. 3 was selected based on simulation results from a sample data set. Specifically, a fully sampled data set was used to simulated different acceleration rates and was also used as a reference for image quality comparisons. The parameter λ was determined by solving the reconstruction problem with different values and choosing the one that minimizes the error with respect to the fully sampled data. To apply the selected λ to a different data set, we normalized the intensity of the data set to have the same intensity of the training data. Note that λ was determined only once and that value was used for all subsequent experiments.

For the experiment with simulated acceleration, coil-by-coil compressed sensing was performed for comparison purposes using the k-t SPARSE method (11), followed by sensitivity-weighted multicoil image combination (32).

Image Analysis

Signal-intensity time courses were evaluated for the reconstructed perfusion images, using two different manually defined regions of interest: one for the entire left ventricle blood pool and one for the entire myocardial wall. The regions of interest were drawn manually, with care to avoid partial-volume effects. The myocardial wall curves were characterized by the baseline (precontrast) mean and standard deviation, peak and upslope. The upslope was computed using a linear fit of the curve points between 10% and 90% of the relative peak enhancement.

Signal intensity profiles along the x dimension were computed using the central line of the images in Fig. 2 at peak blood enhancement. The spatial profiles were characterized by the myocardial wall signal intensity to assess the effect of spatial blurring on the myocardial wall signal before contrast agent arrival and by the signal intensity gradient between myocardial wall and left ventricle to assess the sharpness of the image. The intensity gradient was computed using a linear fit of the points between 20% and 80% of the signal increase from myocardial wall to left ventricle.

For the in vivo study with simulated acceleration, the root mean square error with respect to the fully sampled Fourier reconstruction was evaluated in a subregion surrounding the heart (indicated by the cropped field of view of the images in Fig. 2) and averaged over all time points. The root mean square error values were

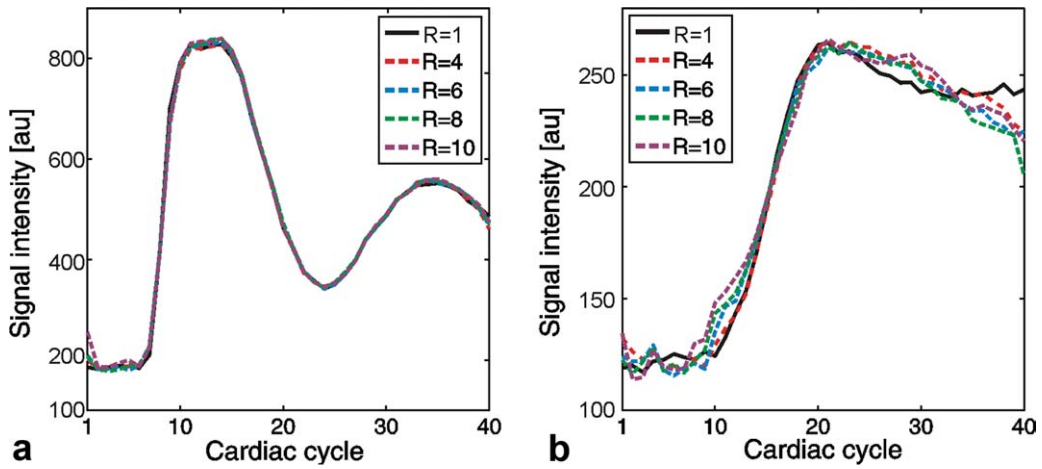

FIG. 3. Signal intensity curves for Fourier reconstruction of the fully sampled data ($R = 1$) and *k-t* SPARSE-SENSE reconstruction with simulated acceleration factors of $R = 4$, 6, 8, and 10: **(a)** blood (left ventricular region of interest) and **(b)** myocardial wall.

expressed as the percentage of the mean value of the fully sampled Fourier reconstruction (x_{full}):

$$RMSE = 100 \times \sqrt{\frac{\sum_{i=1}^{n} \left| x_{acc}(i) - x_{full}(i) \right|^2}{\sum_{i=1}^{n} \left| x_{full}(i) \right|^2}}, \qquad [4]$$

where x_{acc} is the compressed sensing accelerated reconstruction and n is equal to the number of pixels in the region of interest times the number of time points.

RESULTS

Breath-Held Single-Slice Experiment With Simulated Acceleration

k-t SPARSE-SENSE presented superior reconstruction performance when compared to coil-by-coil compressed sensing (Fig. 2). Coil-by-coil compressed sensing root mean square error values were 5.3%, 7.9%, 10.5%, and 14.4%, whereas *k-t* SPARSE-SENSE root mean square error values were 4.6%, 5.7%, 6.5%, and 7.8% for $R = 4$, 6, 8, and 10, respectively. The myocardial wall signal intensity at peak blood (expressed in arbitrary units) was 177.9 for the fully sampled Fourier reconstruction; coil-by-coil compressed sensing values were 206.6, 223.9, 288.2, and 348.8, whereas *k-t* SPARSE-SENSE values were 175.9, 188.2, 188.1, and 244.9 for $R = 4$, 6, 8, and 10, respectively. The intensity gradient between myocardial wall and left ventricle expressed in arbitrary units per pixel was 262.1 for the fully sampled Fourier reconstruction; coil-by-coil compressed sensing values were 239.3, 183.8, 174.1, and 109.2, whereas *k-t* SPARSE-SENSE values were 260.4, 258.9, 242.1, and 190.2 for $R = 4$, 6, 8, and 10, respectively. The increase in the myocardial wall intensity before contrast agent arrival and the decrease in the intensity gradient were produced by spatial and temporal blurring, which were more significant for coil-by-coil compressed sensing.

The maximum compression ratio provided by the temporal FFT was found to be approximately 18, resulting in predicted maximum acceleration factors between 3.6 and 6, using compressed sensing alone. Coil-by-coil compressed sensing resulted in an adequate reconstruction for $R = 4$, in agreement with previous results (15) and theoretical estimates; however, reconstruction artifacts such as spatiotemporal blurring and residual pseudonoise were more noticeable for $R = 6$ and increased in prominence with increasing acceleration. Note that low spatiotemporal frequency components result in sparse coefficients with high values, which can be recovered even at high accelerations. On the other hand, high spatiotemporal frequency components present much lower values in the sparse domain, which fall below the pseudonoise level, and therefore they are more difficult to recover. *k-t* SPARSE-SENSE presented adequate image quality up to $R = 8$, which represents a 2-fold increase over compressed sensing alone.

Figure 3 shows the signal intensity time courses for the blood and myocardial wall for *k-t* SPARSE-SENSE at different acceleration factors, and Table 1 lists the baseline mean and standard deviation, peak, and upslope estimated from the myocardial signal time course. The blood enhancement presented similar temporal fidelity for all accelerations, except for a small amplification of the baseline variation and peak value for higher accelerations. For the myocardial signal-time curve, the mean baseline and peak values were very similar for all accelerations. On the other hand, the baseline variation increased with acceleration due to the higher pseudonoise

Table 1
Baseline Mean Value ± Standard Deviation, Peak Value, and Upslope From the Myocardial Wall Signal Intensity Time Courses for Fourier Reconstruction of the Fully Sampled Data ($R = 1$) and *k-t* SPARSE-SENSE Reconstruction With Different Simulated Acceleration Factors (R)

R	Baseline (au)	Peak (au)	Upslope (au/sec)
1	120.6 ± 2.8	264.6	14.6
4	120.2 ± 4.6	261.9	14.3
6	122.5 ± 5.9	262.3	13.4
8	123.6 ± 7.9	264.6	13.1
10	125.6 ± 10.7	266.3	12.0

au: arbitrary unit

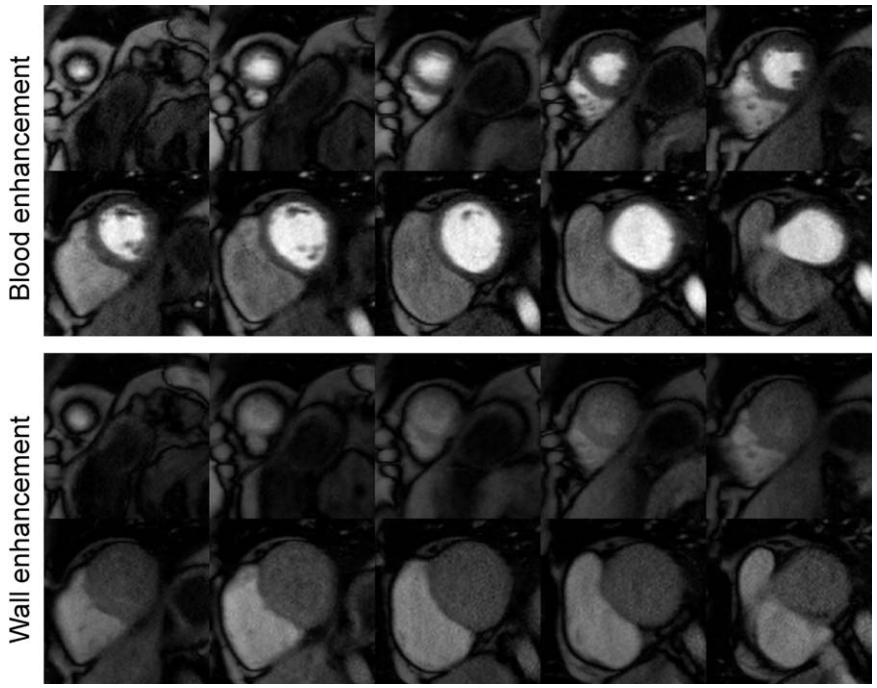

FIG. 4. Breath-held, 8-fold accelerated images in 10 short-axis views at peak blood and peak myocardial wall enhancement. These *k-t* SPARSE-SENSE reconstructed images exhibited good image quality.

level, and the upslope decreased with acceleration due to a small loss of high temporal frequencies in the reconstructed images. The upslope decrease with respect to the fully sampled reconstruction was 2.0%, 8.2%, 10.3%, and 17.8% for $R = 4$, 6, 8, and 10, respectively.

Breath-Held Multislice Experiment With True 8-Fold Acceleration

Figure 4 shows the reconstructed images (10 slices) for the peak blood and peak myocardial wall enhancement phases from the *k-t* SPARSE-SENSE reconstruction of the in vivo breath-held experiment with true 8-fold acceleration. The reconstructed images covered most of the heart, with adequate blood and myocardial wall enhancement and good image quality. The reconstruction time per slice was approximately 15 min, which represented a total reconstruction time of approximately 2.5 h for the 10 slices using MatLab (The MathWorks) on a 64-bit quad core workstation.

Free-Breathing Multislice Experiment With True 8-Fold Acceleration

Figure 5 shows the reconstructed images (10 slices) for the peak blood and peak myocardial wall enhancement time points from the *k-t* SPARSE-SENSE reconstruction of the in vivo experiment with heavy breathing. The reconstruction did not show significant residual incoherent artifacts but did show blurring due to a small loss of sparsity in the temporal Fourier domain. The presence of respiratory motion at higher temporal frequencies than the passage of the contrast agent produces extra low-energy components in the temporal Fourier domain, which are more difficult to recover since they are submerged beneath the pseudonoise created by the incoherent artifacts.

Comparison of k-t SPARSE-SENSE With $R = 8$ and GRAPPA With $R = 2$

Figure 6 shows corresponding images for GRAPPA with $R = 2$ and *k-t* SPARSE-SENSE with $R = 8$. Spatial resolution and blood and myocardial wall enhancement were similar for both methods, but *k-t* SPARSE-SENSE data acquisition was 4-fold higher in temporal resolution and visually presented lower noise amplification in the reconstructed images. Note that true noise also accumulates incoherently in the sparse domain with low-value coefficients. The combination of *k-t* SPARSE and SENSE presents a regularized solution to the inverse problem, where only the high-value sparse coefficients are recovered and the low-value combined true noise and pseudonoise coefficients are neglected. This effectively reduces the noise in the reconstructed images.

Patient Study

Figure 7 shows 8-fold accelerated perfusion images at peak myocardial wall enhancement in three short-axis locations (mid to apical) with perfusion defects. The corresponding phase-sensitive inversion recovery delayed-enhancement images show myocardial infarction regions that correlate well with the perfusion defect regions.

DISCUSSION

The high degree of spatiotemporal correlation in the cardiac perfusion data allows for the application of compressed sensing to accelerate data acquisition. When multiple receiver coils are available, the extra correlation between coils can be exploited to obtain higher accelerations. In this work, a combination of compressed sensing and parallel imaging using the SENSE model and the *k-t* SPARSE method was employed to substantially increase

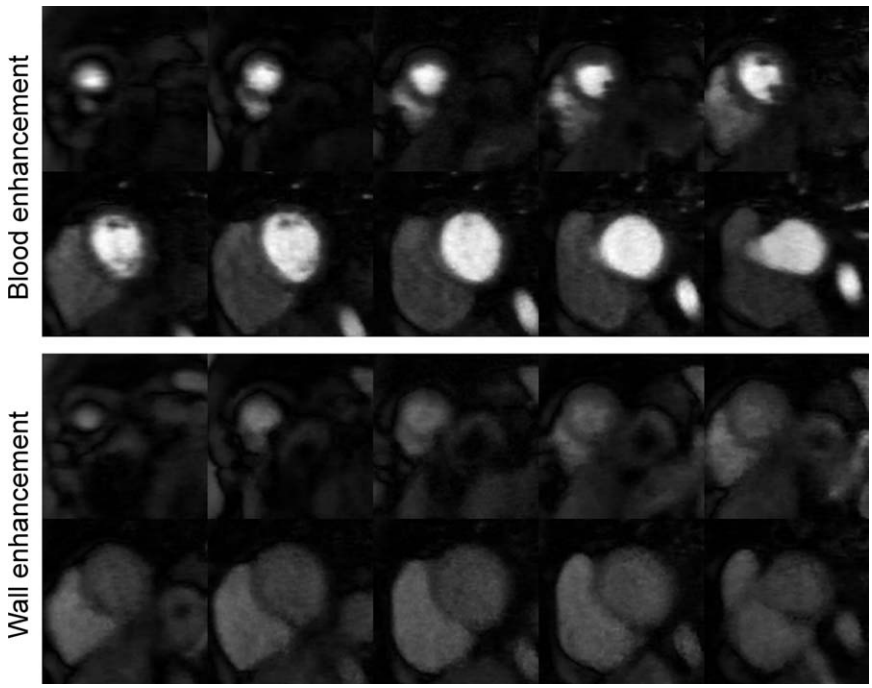

FIG. 5. Free-breathing, 8-fold accelerated images in 10 short-axis views at peak blood and myocardial wall enhancement. These *k-t* SPARSE-SENSE reconstructed images are free of residual aliasing artifacts, but at the expense of a moderate loss in spatiotemporal resolution.

the spatiotemporal resolution and spatial coverage of first-pass cardiac perfusion MRI studies.

Understanding the combined reconstruction from the perspective of distributed compressed sensing theory offers a means to assess theoretical bounds for expected increases in acceleration for combined techniques over each technique applied separately. For example, in this work a 2-fold increase in acceleration over compressed sensing alone was accomplished by using the combined reconstruction with a 12-element coil array, which represents 40-67% of the maximum feasible increase in acceleration for a very large number of coils.

The combination of *k-t* SPARSE and SENSE presented here shares with previously developed *k-t* acceleration methods the use of sparsity in the combined spatial (*x-y*) and temporal frequency (*f*) domain to reconstruct undersampled data. However, these techniques exploit sparsity differently. Methods such as *k-t* SENSE and SPEAR exploit regularities in the sparse domain to reduce signal overlap due to regularly undersampled data, whereas *k-t* SPARSE-SENSE exploits irregularities in the sparse domain to produce undersampling artifacts as pseudonoise that adds incoherently to the sparse representation. *k-t* SENSE and SPEAR perform a linear reconstruction, where the aliased image is unfolded using the signal distribution in *y-f* domain and coil sensitivity information. SPEAR solves the same reconstruction problem as *k-t* SENSE, except for the baseline signal, where a model-based reconstruction using the educed-encoding imaging by

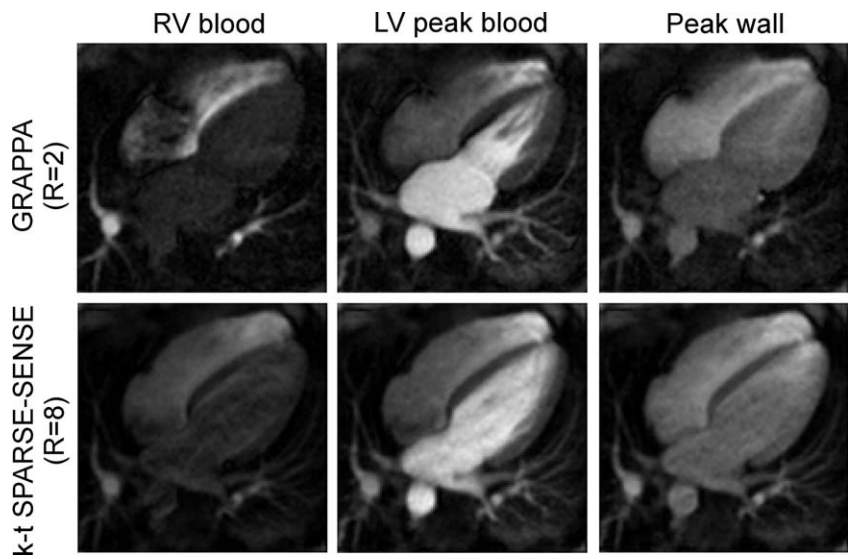

FIG. 6. In vivo comparison of *k-t* SPARSE-SENSE with $R = 8$ and commercially available GRAPPA with $R = 2$ at different points in the contrast update time course.

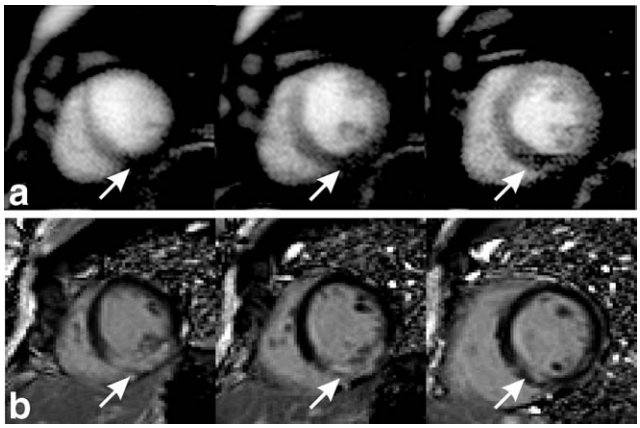

FIG. 7. **a:** Eight-fold accelerated perfusion images at peak myocardial wall enhancement using the combination of *k-t* SPARSE and SENSE. These three selective planes show perfusion defects. **b:** Corresponding phase-sensitive inversion recovery delayed-enhancement images showing myocardial scarring regions that correlate well with the perfusion defect regions.

generalized-series reconstruction (RIGR) algorithm is used instead of the temporal average in order to increase the temporal resolution of *k-t* SENSE. On the other hand, *k-t* SPARSE-SENSE performs a nonlinear reconstruction, where the sparse coefficients are recovered from the interference created by the incoherent undersampling artifacts. Note that *k-t* SPARSE-SENSE does not require training data as explicit knowledge of the particular sparse representation in *y-f* space is not required. Reconstruction artifacts in *k-t* SENSE and SPEAR appear as unfolding errors, whereas artifacts in *k-t* SPARSE-SENSE appear as residual pseudonoise. As a result, *k-t* SPARSE-SENSE may reduce image artifacts due to respiratory motion.

The method used in this work is more closely related to other compressed sensing techniques proposed for dynamic MRI, such as *k-t* SPARSE and *k-t* FOCUSS. However, *k-t* SPARSE-SENSE exploits joint sparsity whereas the other methods exploit single coil sparsity. As a result, the method used in this work provides increased acceleration capability. Moreover, the reconstruction algorithm used here differs from that of *k-t* FOCUSS. *k-t* FOCUSS first produces an initial signal estimate with high temporal resolution, using a model-based reconstruction (RIGR algorithm, as in the SPEAR method), and then enforces sparsity on the remaining part of the signal. As a result, *k-t* FOCUSS may become particularly sensitive to errors in the initial estimate. Another difference is that l_1-norm minimization in *k-t* FOCUSS is approximated by a series of l_2-norm minimization problems with different weights (reweighted l_2-norm), which might require more samples than using a nonlinear algorithm.

Image reconstruction artifacts for higher accelerations include spatiotemporal blurring, attenuation of low-contrast features, and increase of combined noise and pseudonoise. Ideally, if the signal is truly sparse, with only a few large coefficients, compressed sensing will recover only the sparse signal coefficients and suppress the combined noise and pseudonoise. However, in practice the signal is only compressible, i.e., it contains a few large coefficients and many small coefficients. *k-t* SPARSE-SENSE tends to suppress low-valued coefficients in the temporal Fourier domain, such as high spatiotemporal frequencies and low-contrast image features, which are below the combined noise and pseudonoise level. Both noise and pseudonoise in the sparse domain increase with acceleration, which also increases the false detection of sparse signal coefficients, and so more noise and pseudonoise coefficients appear in the solution. However, the filtering of noise coefficients in the sparse domain effectively reduces the noise level in the reconstructed images, at the expense of changing the noise distribution when compared to standard parallel imaging techniques.

The maximum acceleration in *k-t* SPARSE-SENSE is determined by the number of sparse coefficients in the temporal Fourier domain and the number of receiver coils. Tailored sparsifying transforms, which jointly weight spatial and temporal dimensions, may offer a higher compression ratio than the temporal Fourier transform, and the use of coil arrays with larger numbers of elements may substantially reduce the number of required samples (26), resulting in improved performance for cardiac perfusion MRI.

The current implementation of k-*t* SPARSE-SENSE performs a sequential slice-by-slice reconstruction. The reconstruction time per slice is about 15 min using MatLab (The MathWorks) on a 64-bit quad core workstation for the imaging parameters used in this work. For whole-heart coverage, eight to 10 slices are required, which represents a total reconstruction time of 2-2.5 h. Parallel computing can be used to reduce the reconstruction time by reconstructing each slice in parallel. We also expect a further reduction with programming optimization, using a standard programming language such as C++.

Compressed sensing reconstruction can also be performed by minimizing the l_0-norm (number of nonzero coefficients), which in theory would require fewer samples than l_1-norm minimization. However, l_0-norm minimization is a combinatorial optimization problem and therefore computationally intensive. Nevertheless, recently developed methods that approximate the l_0-norm minimization problem have demonstrated fast and stable reconstruction for highly sparse data sets (26,34), and they may be applicable to the combination of compressed sensing and parallel imaging for first-pass cardiac perfusion MRI.

One limitation of the proposed method is the selection of the weighting parameter (λ). In the current implementation, we did not apply any rigorous mathematical criteria to select lambda systematically. Instead, the parameter λ was selected based on simulation results from a single fully sampled data set. Mathematical tools, such as the L-curve, can be used to select λ in a systematic way for an adequate balance between signal-to-noise ratio and spatial-temporal smoothing.

CONCLUSIONS

We have presented a technique combining compressed sensing and parallel imaging for highly accelerated cardiac perfusion MRI. This approach exploits joint sparsity

of the multicoil images in *x-y-f* space. A new theoretical framework for combined reconstruction based on distributed compressed sensing theory was presented to provide estimates of theoretical bounds for feasible accelerations. An in vivo acceleration factor of 8 was feasible with the combined approach, using a 12-element coil array while preserving image quality and temporal fidelity. The combined reconstruction does not require dynamic training data and is relatively insensitive to respiratory motion artifacts. Even higher acceleration rates may be feasible with tailored space-time sparsifying transforms, use of cardiac coil arrays with larger numbers of elements, and four-dimensional acquisitions.

ACKNOWLEDGMENTS

This work was supported by a New York University/Polytechnic Institute of NYU seed grant. The authors thank Ivan Selesnick, Yao Wang, and Jian Xu for helpful discussions. We also thank Robert Donnino for help with the patient study.

REFERENCES

1. Atkinson DJ, Burstein D, Edelman RR. First-pass cardiac perfusion: evaluation with ultrafast MR imaging. Radiology 1990;174:757–762.
2. Barkhausen J, Hunold P, Jochims M, Debatin JF. Imaging of myocardial perfusion with magnetic resonance. J Magn Reson Imaging 2004; 19:750–757.
3. Kellman P, Epstein FH, McVeigh ER. Adaptive sensitivity encoding incorporating temporal filtering (TSENSE). Magn Reson Med 2001; 45:846–852.
4. Breuer FA, Kellman P, Griswold MA, Jakob PM. Dynamic autocalibrated parallel imaging using temporal GRAPPA (TGRAPPA). Magn Reson Med 2005;53:981–985.
5. Tsao J, Boesiger P, Pruessmann KP. k-t BLAST and k-t SENSE: dynamic MRI with high frame rate exploiting spatiotemporal correlations. Magn Reson Med 2003;50:1031–1042.
6. Huang F, Akao J, Vijayakumar S, Duensing GR, Limkeman M. Huang F, Akao J, Vijayakumar S, Duensing GR, Limkeman M. k-t GRAPPA: a k-space implementation for dynamic MRI with high reduction factor. Magn Reson Med 2005;54:1172–1184.
7. Xu D, King KF, Liang ZP. Improving k-t SENSE by adaptive regularization. Magn Reson Med 2007;57:918–930.
8. Gebker R, Jahnke C, Paetsch I, Schnackenburg B, Kozerke S, Bornstedt A, Fleck E, Nagel E. MR myocardial perfusion imaging with k-space and time broad-use linear acquisition speed-up technique: feasibility study. Radiology 2007;245:863–871.
9. Plein S, Ryf S, Schwitter J, Radjenovic A, Boesiger P, Kozerke S. Dynamic contrast-enhanced myocardial perfusion MRI accelerated with k-t SENSE. Magn Reson Med 2007;58:777–785.
10. Jung B, Honal M, Hennig J, Markl M. k-t space accelerated myocardial perfusion. J Magn Reson Imaging 2008;28:1080–1085.
11. Lustig M, Donoho D, Pauly JM. Sparse MRI: the application of compressed sensing for rapid MR imaging. Magn Reson Med 2007; 58:1182–1195.
12. Lustig M, Santos JM, Donoho DL, Pauly JM. k-t SPARSE: high frame rate dynamic MRI exploiting spatio-temporal sparsity. In: Proceedings of the 14th Annual Meeting of ISMRM, Seattle, 2006. p 2420.
13. Gamper U, Boesiger P, Kozerke S. Compressed sensing in dynamic MRI. Magn Reson Med 2008;59:365–373.
14. Jung H, Sung K, Nayak KS, Kim EY, Ye JC. k-t FOCUSS: a general compressed sensing framework for high resolution dynamic MRI. Magn Reson Med 2009;61:103–116.
15. Vitanis V, Manka R, Gamper U, Boesiger P, Kozerke S. Compressed sensing cardiac perfusion imaging. In: Proceedings of the 16th Annual Meeting of International Society for Magnetic Resonance in Medicine (ISMRM), Toronto, 2008. p 2937.
16. Tsaig Y, Donoho DL. Extensions of compressed sensing. Signal Process 2006;86:533–548.
17. Sodickson DK, Manning WJ. Simultaneous acquisition of spatial harmonics (SMASH): fast imaging with radiofrequency coil arrays. Magn Reson Med 1997;38:591–603.
18. Pruessmann KP, Weiger M, Scheidegger MB, Boesiger P. SENSE: sensitivity encoding for fast MRI. Magn Reson Med 1999;42:952–962.
19. Griswold MA, Jakob PM, Heidemann RM, Nittka M, Jellus V, Wang J, Kiefer B, Haase A. Generalized autocalibrating partially parallel acquisitions (GRAPPA). Magn Reson Med 2002;47:1202–1210.
20. Zhao C, Lang T, Jim J. Compressed sensing parallel imaging. In: Proceedings of the 16th Annual Meeting of ISMRM, Toronto, 2008. p 1478.
21. Wu B, Millane RP, Watts R, Bones P. Applying compressed sensing in parallel MRI. In: Proceedings of the 16th Annual Meeting of ISMRM, Toronto, 2008. p 1480.
22. King KF. Combining compressed sensing and parallel imaging. In: Proceedings of the 16th Annual Meeting of ISMRM, Toronto, 2008. p 1488.
23. Liu B, Sebert F, Zou Y, Ying L. SparseSENSE: randomly-sampled parallel imaging using compressed sensing. In: Proceedings of the 16th Annual Meeting of ISMRM, Toronto, 2008. p 3154.
24. Liang D, Liu B, Wang J, Ying L. Accelerating SENSE using compressed sensing. Magn Reson Med 2009;62:1574–1584.
25. Duarte MF, Sarvotham S, Baron D, Wakin MB, Baraniuk RG. Distributed compressed sensing of jointly sparse signals. In: Proceedings of the 39th Conference on Signals, Systems and Computation, Asilomar, 2005. p 1537–1541.
26. Otazo R, Sodickson DK. Distributed compressed sensing for accelerated MRI. In: Proceedings of the 17th Annual Meeting of ISMRM, Hawaii, 2008. p 378.
27. Liang D, King KF, Liu B, Ying L. Accelerating SENSE using distributed compressed sensing. In: Proceedings of the 17th Annual Meeting of ISMRM, Hawaii, 2008. p 377.
28. Seiberlich N, Breuer FA, Blaimer M, Barkauskas K, Jakob PM, Griswold MA. Non-Cartesian data reconstruction using GRAPPA operator gridding (GROG). Magn Reson Med 2007;58:1257–1265.
29. Kim D, Gonen O, Oesingmann N, Axel L. Comparison of the effectiveness of saturation pulses in the heart at 3T. Magn Reson Med 2008;59:209–215.
30. Kim D. Influence of the k-space trajectory on the dynamic T1-weighted signal in quantitative first-pass cardiac perfusion MRI at 3T. Magn Reson Med 2008;59:202–208.
31. Kellman P, Arai AE, McVeigh ER, Aletras AH. Phase-sensitive inversion recovery for detecting myocardial infarction using gadolinium-delayed hyperenhancement. Magn Reson Med 2002;47: 372–383.
32. Roemer PB, Edelstein WA, Hayes CE, Souza SP, Mueller OM. The NMR phased array. Magn Reson Med 1990;16:192–225.
33. Pruessmann KP, Weiger M, Börnert P, Boesiger P. Advances in sensitivity encoding with arbitrary k-space trajectories. Magn Reson Med 2001;46:638–651.
34. Trzasko J, Manduca A. Highly undersampled magnetic resonance image reconstruction via homotopic l(0)-minimization. IEEE Trans Med Imaging 2009;28:106–121.